Organic & Biomolecular Chemistry

ROYAL SOCIETY OF CHEMISTRY

PAPER

View Article Online
View Journal | View Issue

Cite this: *Org. Biomol. Chem.*, 2021, **19**, 3016

Selective photoredox direct arylations of aryl bromides in water in a microfluidic reactor†

Francesca Pallini,[a] Elena Sangalli,[a] Mauro Sassi,[b] Philippe M. C. Roth,[c] Sara Mattiello *[b] and Luca Beverina *[b]

Received 11th January 2021,
Accepted 15th March 2021

DOI: 10.1039/d1ob00050k

rsc.li/obc

Carrying out photoredox direct arylation couplings between aryl halides and aryls in aqueous solutions of surfactants enables unprecedented selectivity with respect to the competing dehalogenation process, thanks to the partition coefficient of the selected sacrificial base. The use of a microfluidic reactor dramatically improves the reaction time, without eroding the yields and selectivity. The design of a metal free sensitizer, which also acts as the surfactant, sizeably improves the overall sustainability of arylation reactions and obviates the need for troublesome purification from traces of metal catalysts. The generality of the method is investigated over a range of halides carrying a selection of electron withdrawing and electron donating substituents.

Introduction

Research on conjugated materials for (opto)electronic applications has historically been dominated by the quest for performances.[1–3] Nowadays, materials exist featuring very promising characteristics for a vast platform of devices, thus promoting industrialization efforts.[4] Such a transition requires the performances to be connected with straightforward, cheap and sustainable synthesis.[5] The fabrication of nearly all polyconjugated materials requires the use of metal catalysts and vast amounts of toxic organic solvents.

Chemists are increasingly realizing that nonaqueous solvents can be replaced by aqueous solutions of micelle forming surfactants, even for the manufacturing of water insoluble organics.[6–8] A vast array of C–C and C–N bond forming reactions are possible, irrespective of the lipophilicity of the reagents and/or products.[9] The key concept of the so-called micellar catalysis approach lies in the preferential accumulation of organics within the lipophilic pockets formed by the various association colloids resulting from the self-assembly of surfactants in aqueous solutions. Thereby, thanks to the particularly high effective concentration and to local polarity effects, reactions are efficient and often selective even at the ppm level of catalyst loading.[10–13]

The choice of the surfactant is crucial. Specifically designed (designer) surfactants ensure efficiency and generality with best performances obtained with the popular tocopherol containing TPGS-750-M[14] introduced by Lipshutz and the proline containing FI-750-M[15] designed by Handa. Industrial surfactants can also be employed. In the case of the PEGylated castor oil derivative Kolliphor EL (K-EL), pronounced oxygen resistance enables use in the standard laboratory environment.[16–19] The adoption of the emerging photoredox direct arylation reactions (PDAs) could further simplify the processes, enabling the direct coupling of an aryl halide with an unactivated aryl partner through a photoinitiated and metal free radical process.

Photoredox reactions in water are already known, yet research is still required to improve selectivity and avoid metal catalysts.[20–25]

In this paper we report the first example of a selective metal free photoinduced direct arylation reaction carried out in water, at room temperature, under a laboratory atmosphere and with negligible competitive dehalogenation. In particular, we show that the unprecedented selectivity is the consequence of the partitioning of the various reactive species in the different compartments of the association colloid formed in water by both K-EL and a specifically devised photoredox mediator (**S-PTh**, Scheme 3) also acting as the cosurfactant.

Results and discussion

Fig. 1 shows the fundamental steps of PDA. The aryl halide (**Ar–X**) is photoreduced to the corresponding radical (**Ar**$^{\bullet}$) by

[a]*University of Milano-Bicocca, Department of Materials Science, via R. Cozzi 55, I-20125 Milan, Italy*

[b]*University of Milano-Bicocca and INSTM, Department of Materials Science, via R. Cozzi 55, I-20125 Milan, Italy. E-mail: sara.mattiello@unimib.it, luca.beverina@unimib.it*

[c]*Corning SAS Reactor Technologies, 7 bis Avenue de Valvins CS 70156 Samois-sur-Seine, F-77210 AVON Cedex, France. E-mail: reactors@corning.com*

†Electronic supplementary information (ESI) available: UV-Vis and electrochemical characterization of the photocatalyst; details of the choice of surfactant; details on photochemical setups and reaction reproducibility; DLS measurements; ^{1}H NMR spectra of new compounds and compounds made with a new procedure. See DOI: 10.1039/d1ob00050k

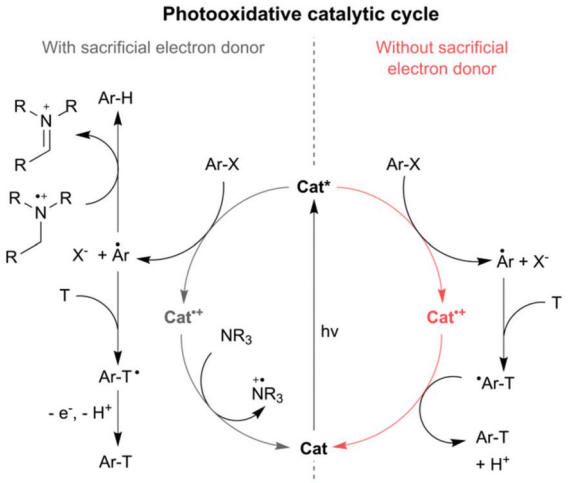

Fig. 1 Photooxidative catalytic cycle proposed in the literature for the formation of the hydrodehalogenation product **Ar–H** and the coupling product **Ar–T** in the presence (grey) or absence (red) of a tertiary amine as a sacrificial electron donor.

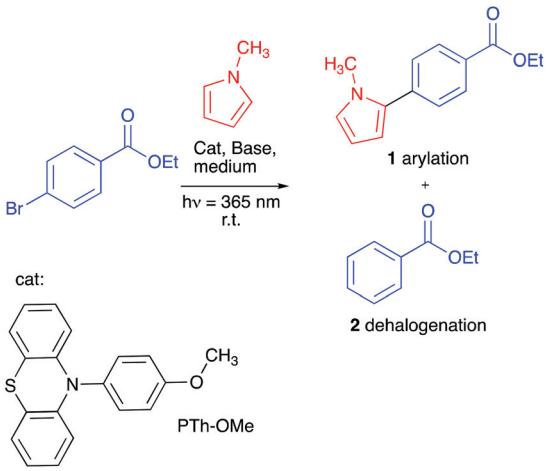

Scheme 1 Photoredox arylation *vs.* dehalogenation in the coupling of ethyl-4-bromobenzoate and *N*-methylpyrrole in the presence of the photoredox catalyst **PTh–OMe**.

the mediator in the excited state (**Cat***). The mediator is reduced back to the ground state (**Cat**) by a sacrificial tertiary amine ($\mathbf{NR_3}$), thus forming the corresponding radical cation ($^{+\bullet}\mathbf{NR_3}$). The $\mathbf{Ar}^{\bullet}$ radical can either intercept the coupling partner (**T**) with subsequent formation of the product (**Ar–T**) or react with $\mathbf{R_3N}^{+\bullet}$ to give the hydrodehalogenation side product (**Ar–H**). The reaction selectively gives **Ar–T** only if **T** is used in large excess (typically 20–50 equivalents), which clearly limits the synthetic usefulness.[26–28] In the absence of $\mathbf{NR_3}$, only the relatively diluted radical $^{\bullet}$**Ar–T** can reduce the **Cat*** intermediate, thus seriously slowing down the reaction (Fig. 1, red pathway).[29] The use of poorly soluble tertiary amines ensures both the presence of the required reducing agent (necessary to regenerate the catalyst) and the swift removal (by precipitation) of the unwanted corresponding radical cation, thus establishing a trade-off between the selectivity and reaction speed.[30] However such an approach requires custom-made amines. The use of micellar catalysis offers a simpler and cheaper alternative.

Aqueous surfactant solutions are microheterogenous environments where hydrophilic, lipophilic and amphiphilic compartments coexist, and chemical species can migrate. Handa has recently demonstrated that reactions having selectivity problems can be dramatically improved by the exploitation of compartmentalization effects limiting the contact between otherwise (in homogeneous phase reactions) freely interacting species.[15,31–33] Pretty much on the same line, we reasoned that the compartmentalization effects, already documented for iridium complex photocatalyzed selective dechlorination,[23] can influence and ultimately control the selectivity of arylation over dehalogenation. Thus, existing evidence supports the hypothesis that the key to selectivity is the efficient removal of the $^{+\bullet}\mathbf{NR_3}$ intermediate from the reaction site, while at the same time ensuring the presence of the parent amine. We here show how, by tuning the experimental conditions in accordance with this hypothesis, efficient PDA in aqueous medium with enhanced selectivity can be achieved.

We selected the arylation of *N*-methyl pyrrole by ethyl-4-bromobenzoate in the presence of the known catalyst 10-(4-methoxy)phenyl-10*H*-phenothiazine (**PTh-OMe**)[34] as the test reaction (Scheme 1). We chose K-EL as the surfactant to ensure stable emulsification, even over very prolonged reaction times. The stability of the emulsions obtained with other popular surfactants, including TPGS-750-M, was comparatively poorer (see the ESI, section 6†). We reduced the excess of the arylation partner from the common 20–50 fold to 5.5 fold in order to highlight the selectivity of the process. To set the baseline, we performed the reaction in a 10 mL cylindrical vial under 365 nm light irradiation (24 h) in a range of organic solvents, using diisopropylethylamine (DIPEA) as the base and comparing the product distribution with respect to the result obtained working in a 2 wt% aqueous K-EL solution (Table 1).

The conversion is generally modest, and the selectivity (*S*) is poor. The use of protic solvents clearly hampers the conversion (EtOH, entry 5). The case of acetone (entry 2) is meaningful, as it supports the previous observation of the role of the solubility of the base employed. Indeed, the DIPEA $^{+\bullet}\mathbf{NR_3}$ radical cation is poorly soluble and precipitates in the reaction mixture, thus partially hampering the dehalogenation pathway.

The reaction in K-EL solution was particularly slow but gave the best selectivity by far.

Indeed, DIPEA is only modestly soluble in water (solubility of 4 g L^{-1}), thus preferentially localizing in the organic phase ($\log P$ = 2.4).‡ Conversely, the $^{+\bullet}\mathbf{NR_3}$ radical cation is an ionic compound, soluble in water. Prior to irradiation, the organic droplets are constituted by the lipophilic bromide, most of the *N*-methylpyrrole ($\log P$ = 1.4)‡ and the photocatalyst. Upon

‡Calculated using Advanced Chemistry Development (ACD/Labs) Software V11.02 (© 1994–2020 ACD/Labs).

Table 1 Composition of the reaction mixture for the coupling of ethyl-4-bromobenzoate with *N*-methylpyrrole performed in different solvents after 24 hours of illumination. Reaction conditions: ethyl-4-bromobenzoate (1 eq.), *N*-methylpyrrole (5.5 eq.), DIPEA (1.5 eq.), **PTh–OMe** (0.05 eq.), *hv* = 365 nm, 36 W. Reactions were performed at 0.1 M concentration of the bromide in the chosen solvent

Entry	Medium	Conversion[a] (%)	Yield of **1**[a] (%)	Yield of **2**[a] (%)	**1** : **2** ratio (*S*)
1	MeCN	50	28	22	1.3
2	Acetone	44	26	16	1.6
3	DMSO	34	19	15	1.3
4	DCM	14	6.5	7	0.9
5	EtOH	3	1	2	0.5
6	2 wt% K-EL	21	14	6.5	2.2

[a] Based on the consumption of bromide according to the GC-MS data.

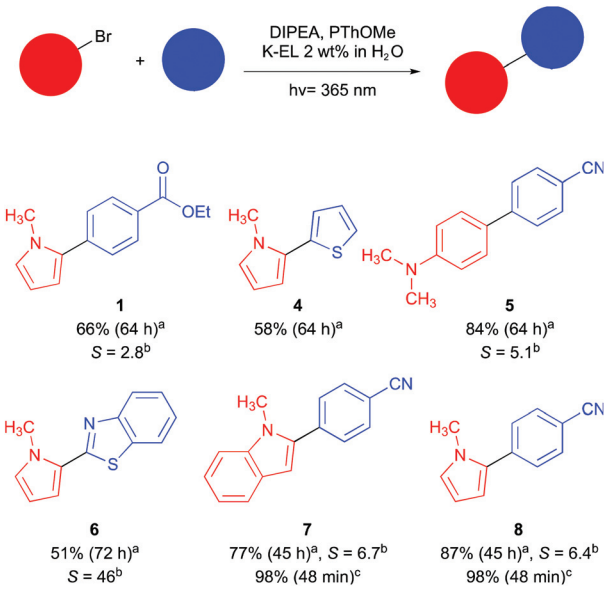

Scheme 2 (a) GC-MS conversion of the bromide in batch reactions performed according to the following method: bromide (blue, 1 eq.), aryl (red, 5.5 eq.), DIPEA (1.5 eq.), **PTh–OMe** (0.1 eq.), *hv* = 365 nm, 36 W. Medium: K-EL 2 wt%. (b) *S* = selectivity, defined as the ratio between arylation over the dehalogenation product based on the GC-MS data. (c) the reaction was performed in the Corning® Lab Photo Reactor using TEA (1.5 eq.) as the base.

irradiation, the $^{+\bullet}$**NR$_3$** salt, produced by the reaction of DIPEA with the photosensitizer radical cation, migrates in the water phase, thus making the dehalogenation pathway sizeably less likely to occur. Fig. 2 shows a graphical representation of the proposed mechanism depending on the base employed. Unfortunately, the improved selectivity comes at the cost of a strongly reduced conversion. The result is not surprising: the reaction mixture is an opaque emulsion where light penetration is minimal. Albeit slow, the reaction has certain generality, and the selectivity of the arylation pathway is always remarkable (Scheme 2). As is generally observed in photoredox arylation under homogeneous conditions, the reaction is particularly efficient in the case of halides featuring electron withdrawing groups at conjugated positions (derivatives **5**, **7** and **8**). Reaction with electron rich bromides such as 2-bromothiophene (derivative **4**) is significantly slower.[28,34] Pyrrole (derivative **8**) is more reactive than indole (derivative **7**) over the same halide. Microfluidic reactors can dramatically improve performances without eroding the synthetic usefulness by means of parallelization of the reaction flasks.[35,36]

The reaction mixture is pumped through microchannels with a high surface-area-to-volume ratio, specifically devised to optimize mixing, thermal exchange and reproducibility. Light

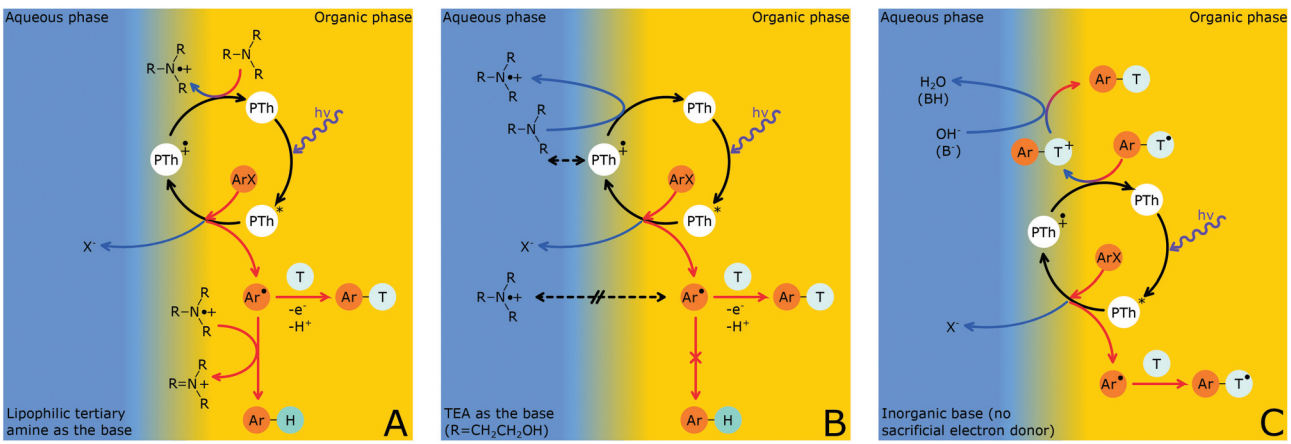

Fig. 2 Cartoon of the accessible paths of the oxidative catalytic cycle in emulsion, depending on the nature of the base employed. (A) Lipophilic tertiary amine: the amine closes the catalytic cycle in the oil phase, thereby turning into $NR_3^{\bullet+}$. Such species localizes preferentially at the aqueous/organic interphase, thus being still able to interact with **Ar**$^\bullet$, and promoting the formation of **Ar–H**. (B) Hydrophilic tertiary amine (like TEA): the catalytic cycle can still be closed by the tertiary amine, but in this case the $NR_3^{\bullet+}$ is hydrophilic and migrates in the aqueous phase, thus being unable to interact with **Ar**$^\bullet$ and form **Ar–H**. (C) No sacrificial electron donor present: the catalytic cycle can only be closed by **Ar–T**$^\bullet$, which transforms into **Ar–T**$^+$, eventually being deprotonated to **Ar–T** in the water phase by the action of a mineral base.

soaking is also dramatically improved even for opaque media, due to the extreme reduction of the optical pathway. A Corning® Lab Photo Reactor is particularly suited for the present study, as it features channels specifically designed to ensure efficient emulsification at all times and reproducibility (see the ESI, section 9†).

Table 2 shows that under comparable experimental conditions the reaction time of the test coupling goes from days to hours in all of the cases. In particular, the reaction performed in MeCN with DIPEA as the base was complete after only 36 minutes (Table 2, entry 2), to be compared with the 49% conversion after 24 hours obtained using the original setup (Table 1, entry 1). Similarly, the reaction in an aqueous surfactant solution performed with DIPEA reached 95% conversion in 2.2 hours (Table 2, entry 6), to be compared with the 21% conversion after 24 h use of the original setup (Table 1, entry 6). Comparison between reactions performed with the same base in MeCN and aqueous medium confirms the trend we observed previously: homogeneous phase reactions are faster but less selective towards the arylation product. Remarkably, the selectivity of the reactions performed in water further improves when DIPEA is replaced with more hydrophilic amines. Even though such a trend can also be observed for the homogeneous phase MeCN reactions, the effect is way more evident in water (Fig. 3), to the point that in the case of triethanolamine (TEA $\log P = -0.99$) product **2** was completely absent (see Fig. S13 of the ESI† for more details on the effect of the base polarity).

Table 2 Coupling of ethyl-4-bromobenzoate and *N*-methylpyrrole performed in the Corning® Lab Photo Reactor. Reaction conditions: ethyl-4-bromobenzoate (1 eq.), *N*-methylpyrrole (5.5 eq.), base (1.5 eq.), PTh–OMe (0.05 eq.), *hv* = 365 nm, 30.5 W. Reactions were performed at 0.1 M formal concentration of bromide

Entry	Medium	Base ($\log P$)[e]	Time (h)	**1** [a] (%)[f]	**2**[a] (%)
1	MeCN	TPA (3.2)	1	70	30
2	MeCN	DIPEA (2.4)	0.6	75	25
3	MeCN	TEtA (1.6)	1	76	20
4[b]	MeCN	TEA (−0.99)	48	31	7
5	2 wt% K-EL	TPA (3.2)	3	75	17
6	2 wt% K-EL	DIPEA (2.4)	2.2	80	15
7	2 wt% K-EL	TEtA (1.6)	2.6	87	7
8	2 wt% K-EL	TEA (−0.99)	3	74	nd
9	2 wt% K-EL	K_3PO_4	3	64	nd
10[c]	2 wt% K-EL/S-PTh	TEA (−0.99)	3	94 (65)[d]	nd

[a] GC-MS data. [b] Batch reaction: precipitation of NEt_3·HBr clogs the microfluidic reactor channels. [c] Reaction performed with 0.1 equivalents of **S-PTh** instead of **PTh–OMe**. [d] Isolated yield. [e] Calculated using Advanced Chemistry Development (ACD/Labs) Software V11.02 (© 1994–2020 ACD/Labs). [f] Due to the low excess of *N*-methylpyrrole employed, formation of a small amount of the double arylation product **3** was observed. Its yield was counted with the yield of product **1** for the evaluation of reaction selectivity.

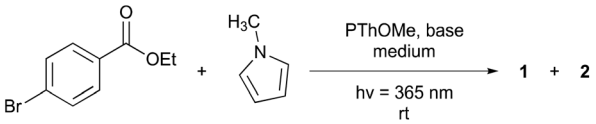

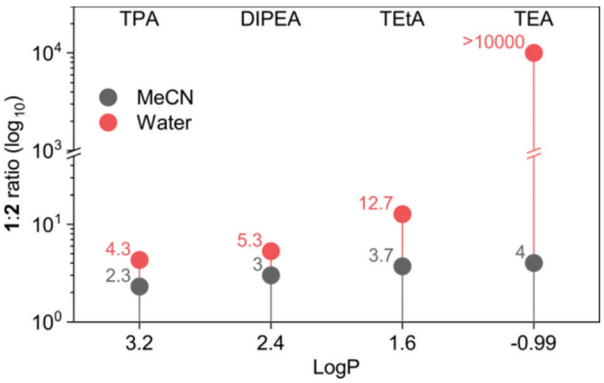

Fig. 3 Selectivity (as the ratio of **1** to **2** product) observed for the test reaction performed in water (red) and acetonitrile (grey) media with different amines.

Raising the temperature at 40 °C did not improve either the conversion or selectivity. Working under the same experimental conditions, we prepared both product **7** and product **8** in 48 min, to be compared with the 45 h required by the original setup (Scheme 2). As localization of the species is key for both selectivity and kinetics, we designed the PEGylated analogue of **PTh–OMe**, **S-PTh**.

The latter can be straightforwardly prepared from **PTh–OMe** in 3 steps using inexpensive reagents (Scheme 3).

The need for the preparation of a specific photoredox active surfactant might be considered as a shortcoming of the method. Yet, the protocol is efficient in terms of both overall yield and sustainability, as **S-PTh** can be isolated on gram scale with an overall *E*-factor (the ratio between the mass of wastes and the mass of the product) of 45, a number in line with scaled up processes in the drug industry.

S-PTh should preferentially localize at the water/oil interphase, where the concentration of the hydrophilic amines such as TEA is higher, thus ensuring a favourable trade-off between speed and selectivity.

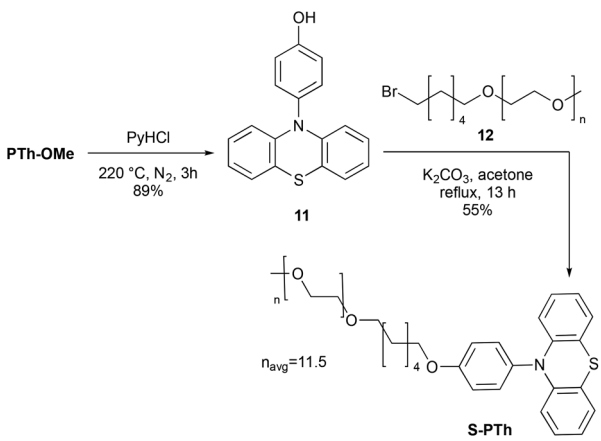

Scheme 3 Synthesis of the photoredox active surfactant **S-PTh**.

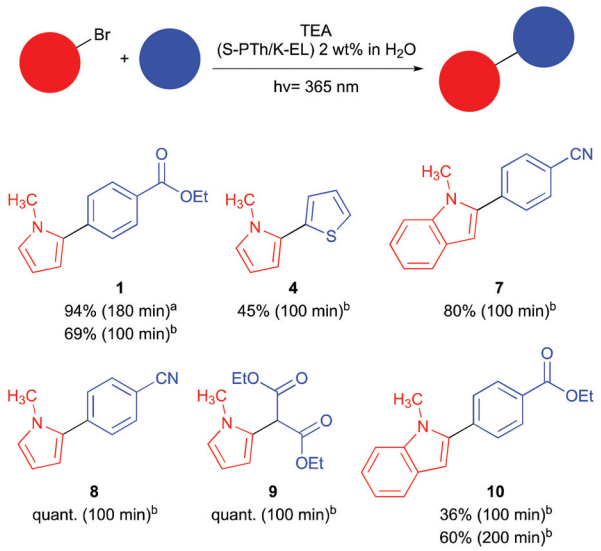

Scheme 4 GC-MS yields of the arylation product in microfluidic photoredox reactions in the presence of the **S-PTh** cosurfactant: (a) Corning® Lab Photo Reactor; and (b) Chemtrix Labtrix® Start reactor.

In a formulation with **K-EL**, **S-PTh** enabled further boost of the conversion to 94% under otherwise identical conditions, while maintaining complete selectivity towards arylation. As shown in Scheme 4, the behaviour is general and robust, even when working with a benchtop microflow setup (Chemtrix Labtrix® Start). Apart from derivative **4**, reflecting the typical low reactivity of 2-bromothiophene in photoredox reactions, the method is very efficient whenever the arylation partner is pyrrole. In the case of indole arylation, reactions become sizeably slower while remaining in any case selective.

Conclusion

In conclusion, we have developed a new method to carry out photopromoted direct arylation reactions in water using a metal free sensitizer. The use of continuous flow photoreactors enabled the achievement of synthetically useful and reproducible results even if the reaction mixture is an opaque emulsion. Flow chemistry allowed us to improve the process compared to batch, and best results were obtained in the scalable Lab Photo Reactor. This reactor allowed fine tuning of the operating conditions and scaling up. The most relevant advantage of our method over competing organic solvent-based protocols is the enhanced selectivity of arylation over the dehalogenation pathway. The result was obtained exploiting an efficient compartmentalization of the reactive species within the distinct phases of the microheterogeneous reaction mixture. A further relevant advantage of the method is the absence of a metal catalyst. Such a feature improves the overall sustainability of arylation reactions and removes the need for the somewhat troublesome purifications required to remove traces of metal catalysts.

Experimental section

General information

Reagents and solvents were bought from TCI, Fluorochem, or Sigma-Aldrich. *N*-Methylpyrrole was distilled under a nitrogen atmosphere before use, and thereafter kept in cold (4 °C) in the dark. Other reagents were used as received. HPLC grade water was used for reactions in emulsion. Chromatographic purification was performed using Davisil LC 60A silica gel (pore size 60 Å, 70–200 μm). Compositions of the solvent mixtures used as eluents are indicated as volume/volume ratios. In the case of test coupling reaction performed between ethyl 4-bromobenzoate and *N*-methylpyrrole, the composition of the reaction mixtures was quantified by quantitative GC-MS through peak integration based on a response factor method (see section 7 of the ESI† for details). For reactions performed on other substrates, the composition of the reaction mixtures was estimated by semiquantitative GC-MS, and eventually quantified by ^{1}H NMR.

GC-MS chromatograms were collected on a Clarus500 PerkinElmer system paired with a Clarus560S mass spectrometer using an Elite-5MS 30.0 m × 250 μm column. Helium was used as the carrier gas. NMR spectra were collected on a Bruker NMR Avance 400 NEO. Melting points were determined using a Buchi M-560 apparatus.

Procedures for the synthesis of the photocatalysts

10-(4-Methoxy)phenyl-10*H*-phenothiazine (PThOMe). Kolliphor ELP (912 mg), phenothiazine (10.000 g, 50.183 mmol), NaOH (3.015 g, 75.37 mmol), ^{t}BuOH (5.590 g, 75.41 mmol), $(^t\text{Bu})_3\text{PHBF}_4$ (587 mg, 2.02 mmol) and $Pd(OAc)_2$ (226 mg, 1.01 mmol) were weighed and put in a 250 mL two-necked round bottom flask equipped with a condenser and a septum. The flask was put under a nitrogen atmosphere and degassed water (45 mL) was added, followed by anhydrous THF (5 mL) and 4-bromoanisole (9.740 g, 52.07 mmol). The mixture was heated and stirred at 60 °C, initially turning into an emulsion. After 1 hour and a half, the mixture became grainy, and a solid formed. After 20 hours, the reaction was stopped, and the reaction mixture was allowed to warm. The solid was filtered on a Büchner funnel and washed with a H_2O/EtOH 1 : 1 solution (40 mL), followed by cold ethanol (20 mL), and finally dried at 60 °C under vacuum. 14.730 g of the product were recovered as a white powder. The product was hot filtered from 330 mL of AcOEt\EtOH 2 : 1, and the filtered solution was left crystallizing at room temperature, and then at −18 °C. 12.550 g of the product were recovered as brownish crystals (81.9% yield). Mp 174–175 °C (lit. 176–177 °C).[37]

^{1}H NMR (400 MHz, benzene-d_6): δ[ppm] 6.95 (dd, J = 7.4, 1.7 Hz, 2H), 6.91 (d, 9.0 Hz, 2H), 6.71–6.64 (m, 4H), 6.59 (td, J = 7.4, 1.4 Hz, 2H), 6.24 (dd, J = 8.1, 1.4 Hz, 2H), 3.24 (s, 3H).

10-(4-Methoxyphenyl)-10*H*-phenothiazine (derivative 11). PTh–OMe powder (7.000 g, 22.92 mmol) and pyridinium chloride (26.480 g, 229.15 mmol) were weighed in a 250 mL two-necked round bottom flask, put under a nitrogen atmosphere and heated and stirred at 200 °C. After 3 hours, the reaction

mixture was warmed to room temperature, and quenched with a 2% $NaHSO_3$ aqueous solution (80 mL). The precipitated product was recovered by filtration, washed with H_2O (100 mL) and finally dried under vacuum. 6.000 g, 89.4% yield. Mp 151–153 °C.

^{1}H NMR (400 MHz, acetone-d_6): δ[ppm] 8.81 (s, 1H), 7.26 (d, J = 8.8 Hz, 2H), 7.14 (d, J = 8.8 Hz, 2H), 7.01 (dd, J = 7.5, 1.7 Hz, 2H), 6.91 (ddd, J = 8.2, 7.3, 1.7 Hz, 2H), 6.83 (td, J = 7.4, 1.3 Hz, 2H), 6.26 (dd, J = 8.2, 1.3 Hz, 2H). ^{13}C NMR (100 MHz, acetone-d_6): δ[ppm] 157.5, 144.8, 132.2, 132.1, 127.0, 126.4, 122.3, 119.4, 117.4, 115.7. Anal. Calcd for $C_{18}H_{13}NOS$: C, 74.20; H, 4.50; N, 4.81. Found: C, 74.42; H, 5.63; N, 4.69.

Derivative 12. MPEG-550 (30.000 g, 54.545 mmol) and NaOH (10.910 g, 272.75 mmol) were weighed in a 250 mL two-necked round bottom flask and put under a nitrogen atmosphere. Water was added (10.910 g) and the reaction mixture was heated to 70 °C. Upon NaOH dissolution, the reaction mixture was cooled to 55 °C and 1,6-dibromohexane (66.500 g, 272.59 mmol) was added. After 24 hours the reaction mixture was allowed to warm to room temperature. The mixture was filtered on glass wool and put in a separating funnel to remove the aqueous phase. 30 mL of Et_2O was added into the funnel, and the product was subsequently washed with a buffer aqueous solution of NaH_2PO_4/Na_2HPO_4 (10%–10%, 30 mL). The organic phase was dried on Na_2SO_4 and filtered, and the solvent was evaporated under reduced pressure. Excess 1,6-dibromohexane was recovered by distillation at 120 °C and 0.1 mbar. 1 L of water was added to the distillation residue to remove dibromohexane traces under steam distillation. Water was evaporated under reduced pressure, and the obtained oil was dissolved in AcOEt (50 mL) and dried on Na_2SO_4. The solution was finally filtered, and AcOEt was evaporated under reduced pressure. 34.770 g of the product were obtained as a colourless viscous liquid (yield 89.5%).

^{1}H NMR (400 MHz, $CDCl_3$): δ[ppm] 3.68–3.63 (m, 40H), 3.60–3.54 (m, 4H), 3.47 (t, J = 6.6 Hz, 2H), 3.42 (t, J = 6.9 Hz, 2H), 3.39 (s, 3H), 1.90–1.84 (m, 2H), 1.64–1.57 (m, 2H), 1.50–1.34 (m, 4H). As the product is a mixture of substances having MPEG chains of different lengths, ^{13}C NMR spectrum was not recorded for this derivative.

Derivative S-PTh. Derivative **11** (2.430 g, 8.340 mmol), **12** (6.000 g, 8.416 mmol) and K_2CO_3 (1.730 g, 12.52 mmol) were weighed and put in a two-necked 250 mL round bottom flask, equipped with a condenser and a septum. The flask was put under a nitrogen atmosphere and degassed acetone (10 mL) was added to the reaction mixture. The reaction mixture was stirred under reflux for 13 hours, and thereafter allowed to cool down to room temperature. The mixture was diluted with acetone (10 mL) and filtered. 8.00 g of silica were added to the solution, following which the solvent was evaporated under reduced pressure, and the obtained powder was extracted in a Soxhlet apparatus with heptane (to remove unreacted **11** and **12**), and subsequently with diisopropyl ether to collect the product. After solvent evaporation, 4.158 g of **S-PTh** were obtained as a brownish viscous oil (yield: 54.7%).

^{1}H NMR (400 MHz, DMSO-d_6) δ[ppm]: 7.32 (d, J = 8.9 Hz, 2H), 7.19 (d, J = 8.9 Hz, 2H), 7.04 (dd, J = 7.5, 1.6 Hz, 2H), 6.91 (ddd, J = 8.2, 7.4, 1.7 Hz, 2H), 6.83 (td, J = 7.4, 1.3 Hz, 2H), 6.14 (dd, J = 8.2, 1.2 Hz, 2H), 4.05 (t, J = 6.4 Hz, 2H), 3.52–3.50 (m, 44H), 3.43–3.39 (m, 4H), 3.24 (s, 3H), 1.80–1.74 (m, 2H), 1.58–1.34 (m, 6H). As the product is a mixture of substances having MPEG chains of different lengths, ^{13}C NMR spectrum was not recorded for this derivative.

The average length of the MPEG chain was estimated by ^{1}H NMR (n_{avg} = 11.5, see Fig. S19†). The average **S-PTh** molecular weight therefore corresponds to 911 g mol^{-1}.

Procedures for the preparation and analysis of photochemical reactions

General procedures for reactions performed in batch. In the case of reactions performed in solvents other than water (see Table 1, entries 1–5), ethyl 4-bromobenzoate (91.9 mg, 0.400 mmol), *N*-methylpyrrole (178 mg, 2.20 mmol), DIPEA (77.7 mg, 0.600 mmol) and **PTh–OMe** (6.11 mg, 0.0200 mmol) were dissolved in the chosen solvent (4 mL). The solution was subsequently irradiated for 24 hours under UV-A light (see section 2.1 of the ESI† for details), at the end of which 0.2 mL of the reaction mixture was diluted with DCM, filtered and subjected to GC-MS analysis.

In the case of reactions performed in water (see Table 1, entry 6, and Scheme 2), a solution of the (hetero)aryl halide (0.400 mmol), the coupling partner (2.20 mmol) and DIPEA (77.7 mg, 0.600 mmol) was emulsified in 4 mL of 2 wt% surfactant aqueous solution by sonication in an ultrasound bath for 15 minutes. In the case of reactions performed using **PTh–OMe**, the catalyst was dissolved in the organic phase and emulsified as well. In the case of reactions performed using **S-PTh**, the catalyst (36 mg, 0.040 mmol) was dissolved in water with the amount of K-EL (44 mg) necessary to obtain a 2 wt% aqueous solution of both surfactants. The emulsified mixture was subsequently irradiated for an appropriate amount of time under UV-A light. Samples for GC-MS analysis were prepared extracting 0.2 mL of the reaction mixture with 2 mL of DCM, and filtering the organic phase on cotton wool to remove water and salt residues.

General procedures for reactions performed with the Corning® Lab Photo Reactor. In the case of reactions performed in acetonitrile (see Table 2, entries 1–4), ethyl 4-bromobenzoate (345 mg, 1.5 mmol), *N*-methylpyrrole (669 mg, 8.25 mmol), the chosen base (2.25 mmol) and **PTh–OMe** (22.9 mg, 0.0750 mmol) were dissolved in 15 mL of acetonitrile. 12 mL of this solution were subsequently recirculated within the reactor under irradiation for an appropriate amount of time (see section 2.2 of the ESI† for details). The remaining 3 mL was used as a reservoir to replenish the reactor after sampling the reaction for GC-MS analysis. Samples for GC-MS analysis were prepared diluting 0.2 mL of the reaction mixture with DCM and filtering the solution with a syringe PTFE filter (0.45 μm).

In the case of reactions performed in water (see Table 2, entries 5–10, and Schemes 2 and 3), the halide (1.50 mmol),

the coupling partner (8.25 mmol) and the chosen base (2.25 mmol) were emulsified in 15 mL of 2 wt% surfactant aqueous solution by sonication in an ultrasound bath for 15 minutes. In the case of reactions performed using **PTh–OMe**, the catalyst was dissolved in the organic phase and emulsified as well. In the case of reactions performed using **S-PTh**, the catalyst (137 mg, 0.150 mmol) was dissolved in water with the amount of K-EL (163 mg) necessary to obtain a 2 wt% aqueous solution of both surfactants. 12 mL of this emulsion were subsequently recirculated within the reactor under irradiation for an appropriate amount of time. The remaining 3 mL were used as a reservoir to replenish the reactor after sampling the reaction for GC-MS analysis. Samples for GC-MS analysis were prepared extracting 0.2 mL of the reaction mixture with 2 mL of DCM, and filtering the organic phase on cotton wool to remove water and salt residues.

*Specifically, in the case of the reaction described in Table 2, entry 10 for the synthesis of product **1**.* 14 mL of the reaction mixture were used out of the 15 mL prepared. At the end of the reaction, water was removed under reduced pressure, and the raw mixture was taken with DCM. The precipitate was filtered, and the crude product was purified by column chromatography using heptane/AcOEt 8 : 2 as the eluent. Isolated product: 209 mg, 65% yield.[38]

^{1}H NMR (400 MHz, $CDCl_3$): δ[ppm] 8.06 (d, J = 8.6 Hz, 2H), 7.47 (d, J = 8.6 Hz, 2H), 6.73 (m, 1H), 6.33 (dd, J = 3.7, 1.8 Hz, 1H), 6.22 (dd, J = 3.7, 2.6 Hz, 1H), 4.39 (q, J = 7.1 Hz, 2H), 3.71 (s, 3H), 1.41 (t, J = 7.1 Hz, 3H).

General procedures for reactions performed with the Chemtrix Labtrix® Start reactor

The procedure applies for the reactions in Scheme 4. A stock solution of **S-PTh** (273 mg, 0.300 mmol) and K-EL (327 mg) in water (30 mL) was prepared and used to perform all the described couplings. The halide (0.1000 mmol), the coupling partner (0.5500 mmol) and the TEA (22.38 mg, 0.1500 mmol) were emulsified in 1 mL of the S-PTh/K-EL aqueous stock solution by sonication in an ultrasound bath for 15 minutes. This emulsion was subsequently injected within the reactor under irradiation at a 0.1 μL min^{-1} flow rate, remaining under illumination for 100 minutes. Samples for GC-MS analysis were prepared extracting 0.2 mL of the reaction mixture with 2 mL of DCM and filtering the organic phase on cotton wool to remove water and salt residues. An analytical sample for each described product was obtained by chromatographic purification of the residual extract.

*Product **4**.* Eluent heptane/DCM 1 : 1.

^{1}H NMR (400 MHz, $CDCl_3$): δ[ppm] 7.27 (dd, J = 5.1, 1.2 Hz, 1H), 7.07 (m, 1H), 7.03 (dd, J = 3.6, 1.1 Hz, 1H), 6.71 (m, 1H), 6.34 (d, J = 3.5 Hz, 1H), 6.18 (m, 1H), 3.73 (s, 3H).[39]

*Product **7**.* Eluent heptane/DCM 1 : 1.

^{1}H NMR (400 MHz, $CDCl_3$): δ[ppm] 7.69 (d, J = 8.4 Hz, 2H), 7.55–7.60 (m, 3H), 7.32 (d, J = 8.3 Hz, 1H), 7.23 (t, J = 7.5 Hz, 1H), 7.10 (t, J = 7.5 Hz, 1H), 6.59 (s, 1H), 3.71 (s, 3H).[40]

*Product **8**.* Eluent toluene/Et_2O 99 : 1.

^{1}H NMR (400 MHz, $CDCl_3$): δ[ppm] 7.67 (d, J = 8.6 Hz, 2H), 7.50 (d, J = 8.6 Hz, 2H), 6.78 (m, 1H), 6.35 (dd, J = 3.7, 1.7 Hz, 1H), 6.23 (dd, J = 3.7, 2.7 Hz, 1H), 3.71 (s, 3H).[27]

*Product **9**.* Eluent heptane/AcOEt 95 : 5.

^{1}H NMR (400 MHz, $CDCl_3$): δ[ppm] 6.61 (t, J = 2.2 Hz, 1H), 6.21 (dd, J = 3.7, 1.7 Hz, 1H), 6.10 (t, J = 3.1 Hz, 1H), 4.71 (s, 1H), 4.20–4.28 (m, 4H), 3.59 (s, 3H), 1.29 (t, 7.1 Hz, 6H).[41]

*Product **10**.* Eluent heptane/AcOEt 95 : 5.

^{1}H NMR (400 MHz, $CDCl_3$): δ[ppm] 8.15 (d, J = 8.4 Hz, 2H), 7.65 (d, J = 7.8 Hz, 1H), 7.60 (d, J = 8.4 Hz, 2H), 7.38 (d, J = 8.3 Hz, 1H), 7.28 (t, J = 7.5 Hz, 1H), 7.16 (t, J = 7.5 Hz, 1H), 6.65 (s, 1H), 4.43 (q, J = 7.1 Hz, 2H), 3.78 (s, 3H), 1.43 (t, J = 7.1 Hz, 3H).[40]

Author contributions

LB and SM contributed to the conceptualization and supervision. FP, SM and PMCR contributed to the writing of the original draft. LB and MS contributed to review and editing. FP, SM and ES performed the investigation. PMCR provided resources.

Conflicts of interest

There are no conflicts to declare.

Acknowledgements

LB, MS, SM and FP gratefully acknowledge financial contribution for MIUR under grants "Dipartimenti di Eccellenza 2017 Project – Materials for Energy" and PRIN2017 BOOSTER (2017YXX8AZ).

Notes and references

1 L. Meng, Y. Zhang, X. Wan, C. Li, X. Zhang, Y. Wang, X. Ke, Z. Xiao, L. Ding, R. Xia, H.-L. Yip, Y. Cao and Y. Chen, *Science*, 2018, **361**, 1094–1098.
2 Y. Liu, C. Li, Z. Ren, S. Yan and M. R. Bryce, *Nat. Rev. Mater.*, 2018, **3**, 913.
3 M.-A. Pan, T.-K. Lau, Y. Tang, Y.-C. Wu, T. Liu, K. Li, M.-C. Chen, X. Lu, W. Ma and C. Zhan, *J. Mater. Chem. A*, 2019, **7**, 20713–20722.
4 R. Po, A. Bernardi, A. Calabrese, C. Carbonera, G. Corso and A. Pellegrino, *Energy Environ. Sci.*, 2014, **7**, 925–943.
5 R. Po, G. Bianchi, C. Carbonera and A. Pellegrino, *Macromolecules*, 2015, **48**, 453–461.
6 B. H. Lipshutz, S. Ghorai and M. Cortes-Clerget, *Chem. – Eur. J.*, 2018, **24**, 6672–6695.
7 B. H. Lipshutz, F. Gallou and S. Handa, *ACS Sustainable Chem. Eng.*, 2016, **4**, 5838–5849.
8 B. H. Lipshutz, *J. Org. Chem.*, 2017, **82**, 2806–2816.

9 S. Ghorai and B. H. Lipshutz, *Aldrichimica Acta*, 2012, **45**, 3.
10 N. Akporji, R. R. Thakore, M. Cortes-Clerget, J. Andersen, E. Landstrom, D. H. Aue, F. Gallou and B. H. Lipshutz, *Chem. Sci.*, 2020, **20**, 3437.
11 S. Handa, B. Jin, P. P. Bora, Y. Wang, X. Zhang, F. Gallou, J. Reilly and B. H. Lipshutz, *ACS Catal.*, 2019, **9**, 2423–2431.
12 E. B. Landstrom, S. Handa, D. H. Aue, F. Gallou and B. H. Lipshutz, *Green Chem.*, 2018, **20**, 3436–3443.
13 S. Handa, J. D. Smith, Y. Zhang, B. S. Takale, F. Gallou and B. H. Lipshutz, *Org. Lett.*, 2018, **20**, 542–545.
14 B. H. Lipshutz, S. Ghorai, A. R. Abela, R. Moser, T. Nishikata, C. Duplais, A. Krasovskiy, R. D. Gaston and R. C. Gadwood, *J. Org. Chem.*, 2011, **76**, 4379–4391.
15 L. Finck, J. Brals, B. Pavuluri, F. Gallou and S. Handa, *J. Org. Chem.*, 2018, **83**, 7366–7372.
16 M. Sassi, S. Mattiello and L. Beverina, *J. Org. Chem.*, 2020, **2020**, 2806–2816.
17 A. Sanzone, A. Calascibetta, E. Ghiglietti, C. Ceriani, G. Mattioli, S. Mattiello, M. Sassi and L. Beverina, *J. Org. Chem.*, 2018, **83**, 15029–15042.
18 S. Mattiello, M. Rooney, A. Sanzone, P. Brazzo, M. Sassi and L. Beverina, *Org. Lett.*, 2017, **19**, 654–657.
19 S. Mattiello, A. Monguzzi, J. Pedrini, M. Sassi, C. Villa, Y. Torrente, R. Marotta, F. Meinardi and L. Beverina, *Adv. Funct. Mater.*, 2016, **26**, 8447–8454.
20 R. Naumann and M. Goez, *Green Chem.*, 2019, **21**, 4470–4474.
21 C. Kerzig, X. Guo and O. S. Wenger, *J. Am. Chem. Soc.*, 2019, **141**, 2122–2127.
22 R. Naumann, F. Lehmann and M. Goez, *Angew. Chem., Int. Ed.*, 2018, **57**, 1078–1081.
23 M. Giedyk, R. Narobe, S. Weiß, D. Touraud, W. Kunz and B. König, *Nat. Catal.*, 2020, **3**, 40–47.
24 F. Eisenreich, E. W. Meijer and A. R. A. Palmans, *Chemistry*, 2020, **26**, 10355–10361.
25 M.-J. Bu, C. Cai, F. Gallou and B. H. Lipshutz, *Green Chem.*, 2018, **20**, 1233–1237.
26 I. Ghosh, T. Ghosh, J. I. Bardagi and B. Konig, *Science*, 2014, **346**, 725–728.
27 I. Ghosh and B. König, *Angew. Chem., Int. Ed.*, 2016, **55**, 7676–7679.
28 S. O. Poelma, G. L. Burnett, E. H. Discekici, K. M. Mattson, N. J. Treat, Y. Luo, Z. M. Hudson, S. L. Shankel, P. G. Clark, J. W. Kramer, C. J. Hawker and J. Read de Alaniz, *J. Org. Chem.*, 2016, **81**, 7155–7160.
29 R. Matsubara, T. Yabuta, U. Md Idros, M. Hayashi, F. Ema, Y. Kobori and K. Sakata, *J. Org. Chem.*, 2018, **83**, 9381–9390.
30 A. Arora and J. D. Weaver, *Org. Lett.*, 2016, **18**, 3996–3999.
31 P. P. Bora, M. Bihani, S. Plummer, F. Gallou and S. Handa, *ChemSusChem*, 2019, **12**, 3037–3042.
32 M. Bihani, P. P. Bora, M. Nachtegaal, J. B. Jasinski, S. Plummer, F. Gallou and S. Handa, *ACS Catal.*, 2019, **9**, 7520–7526.
33 J. D. Smith, T. N. Ansari, M. P. Andersson, D. Yadagiri, F. Ibrahim, S. Liang, G. B. Hammond, F. Gallou and S. Handa, *Green Chem.*, 2018, **20**, 1784–1790.
34 E. H. Discekici, N. J. Treat, S. O. Poelma, K. M. Mattson, Z. M. Hudson, Y. Luo, C. J. Hawker and J. R. de Alaniz, *Chem. Commun.*, 2015, **51**, 11705–11708.
35 F. Politano and G. Oksdath-Mansilla, *Org. Process Res. Dev.*, 2018, **22**, 1045–1062.
36 S. Santoro, F. Ferlin, L. Ackermann and L. Vaccaro, *Chem. Soc. Rev.*, 2019, **48**, 2767–2782.
37 J.-H. Huang and K.-C. Lee, *ACS Appl. Mater. Interfaces*, 2014, **6**, 7680–7685.
38 E. T. Nadres, A. Lazareva and O. Daugulis, *J. Org. Chem.*, 2011, **76**, 471–483.
39 F. Yu, R. Mao, M. Yu, X. Gu and Y. Wang, *J. Org. Chem.*, 2019, **84**, 9946–9956.
40 Y. Huang, Z. Lin and R. Cao, *Chem. – Eur. J.*, 2011, **17**, 12706–12712.
41 C. Bottecchia, R. Martín, I. Abdiaj, E. Crovini, J. Alcazar, J. Orduna, M. J. Blesa, J. R. Carrillo, P. Prieto and T. Noël, *Adv. Synth. Catal.*, 2019, **361**, 945–950.